AN ACOUSTIC BASED LOCAL POSITIONING SYSTEM FOR DYNAMIC UAV IN GPS-DENIED ENVIRONMENTS

Lok Wai Jacky Tsay[1,2,3], Shiigi Tomoo[4], Zichen Huang[3,*], Hiroaki Nakanishi[5], Tetsuhito Suzuki[6], Keiichiro Shiraga[3], Yuichi Ogawa[3], Naoshi Kondo[3]

[1] Department of Computer Science and Engineering, Shanghai Jiao Tong University, Shanghai, China.
[2] Primeton Information Technologies, Inc., Shanghai, China.
[3] Graduate School of Agriculture, Kyoto University, Kyoto, Japan.
[4] Department of Ocean Mechanical Engineering, National Fisheries University, Shimonoseki, Japan.
[5] Graduate School of Engineering, Kyoto University, Kyoto, Japan.
[6] Laboratory of Productive Environment System, Graduate School of Bioresources, Mie University, Tsu, Mie, Japan.
[*] Correspondence: huang.zichen.22c@kyoto-u.jp

HIGHLIGHTS

- A positioning system for mobile UAVs is needed in a GPS-denied environment.
- A Doppler shift compensation algorithm was proposed.
- The successful detection rate and positioning errors were 90.2% and 75.9 ± 39.1 mm, respectively.
- The system performance meets the requirements for mobile UAVs in an indoor environment.

ABSTRACT. *An alternative positioning system, the Spread Spectrum Sound-based Local Positioning System (SSSLPS), was developed to extend the usage of UAVs in GPS-denied environments, such as greenhouses. To date, it has been proven that the SSSLPS could provide a centimeter-level locational accuracy of static objects and dynamic ground robots. In this research, the ranging and positioning performance of SSSLPS were evaluated with the system mounted on a UAV. Meanwhile, to minimize the Time of Arrival (ToA) estimation error and improve positioning accuracy, a novel Doppler shift compensation algorithm was proposed. Experiments were conducted, and the measurement accuracy was evaluated by comparing the measurement of the motion capture system. The results show a successful detection rate of 90.2% using the proposed algorithm and a position error of 75.9 mm. These results demonstrate that the SSSLPS with spectrum peak algorithm can improve positioning accuracy and enable the SSSLPS to be an accurate positioning system for UAVs in a greenhouse.*

Keywords. *Dopper shift, Greenhouse robots, Positioning system, ToA estimation, UAV.*

Recent greenhouse robotic systems are beginning to incorporate unmanned aerial vehicles (UAV) in order to perform various tasks more efficiently (Simon et al., 2018), such as measuring (Roldán et al., 2015) and mapping (Roldán et al., 2016) greenhouse environmental variables, indoor livestock management (Krul et al., 2021), and yield estimation via tomato flower detection (Oppenheim et al., 2017). In the absence of UAVs, most of these tasks are manually performed, which depends on the skills and availability of workers. In order to relinquish such tasks to automated agricultural robotic systems, the positioning system (navigation) plays a crucial role in guiding robotic motion and coordinating tasks. This is important in indoor environments, such as a greenhouse, where GPS-based positioning systems often cannot operate effectively.

There are other types of positioning systems that can be used in these GPS-denied environments. Ultra-wideband (UWB) is the most famous commercial indoor positioning system with an accuracy of 10 cm (Landolsi, 2017; De Preter et al., 2018). However, a high-frequency signal must be emitted to obtain a high positioning accuracy, which raises a high-cost issue (Gu et al., 2009; Ridolfi et al., 2021). Simultaneous localization and mapping (SLAM), a vision-based indoor positioning method using a monocular camera or RGB-D sensor mounted on a quadcopter (Xiao et al., 2020), has also been explored. It can guide the path of a quadcopter flying in a greenhouse to within an accuracy of 0.16 m (Krul et al., 2021). A hybrid navigation system that applied a sensor fusion algorithm to combine visual-IMU-wheel odometry was proposed for a greenhouse robot, and achieved decimeter level accuracy (Yan et al., 2022). However, SLAM-based localization methods can be challenging if the features in a greenhouse is weakly featured or if features are changing. Nevertheless, Zhang et al. (2022) succeeded in achieving a superior level of positioning performance, with a standard deviation of less than 0.05m, through the application of an artificial feature augmentation approach. There were also navigation systems that set markers in the

Submitted for review on 9 October 2022 as manuscript number ITSC 15397; approved for publication as a Research Article by Associate Editor Prof. Brian Steward and Community Editor Dr. Seung-Chul Yoon of the Information Technology, Sensors, & Control Systems Community of ASABE on 7 May 2023.

environment to guide the UAV's path and landing (Sani and Karimian, 2017). The choice of the positioning system in a greenhouse should balance operational objectives and costs.

Our team has been researching a low-cost, and high-accuracy positioning system based on a spectrum spread sound-based local positioning system (SSSLPS) for the unmanned ground vehicle (UGV) in the greenhouse. As an alternative indoor positioning system, this system is based on similar principles to that of a GPS. Rather than satellites emitting radio waves, multiple sound emitters are set up in the greenhouse, and a receiver is placed on the robot. We have already established, with a wire-linked system in a greenhouse, that a positioning system with a centimeter-level accuracy and acoustic noise tolerance can be achieved over a 12 × 6 m area (Huang et al., 2020b). While other studies have demonstrated that the acoustic noise generated by a stationary quadcopter with a 9.7 N thrust could increase the positioning error by 10 mm in a greenhouse, it has been shown that the noise tolerance of the sound signal can be improved by the use of modulation methods (Huang et al., 2020b). Although there are acoustic-based positioning systems available on the market, such as Marvelmind (Tallinn, Estonia), these systems are not specifically designed for use with greenhouse robots, which require additional settings to address unique environmental challenges such as microclimate (Shiigi et al., 2017) and environmental noise (Widodo et al., 2014). In contrast, the movement of a low-noise crawler robot can compensate for a Doppler shift effect by extracting the carrier wave (Huang et al., 2021). The objectives are to address the two separate issues, namely the noise and the Doppler shift effect, of a sound-based navigation system on a dynamically moving UAV that will be used to perform machine vision analysis for monitoring plants in a greenhouse environment.

We proposed a novel Doppler shift compensation algorithm that selects the strongest correlation SNR signal from a series of correlation signals calculated using candidate Doppler shifted reference signals to obtain an accurate Time of Arrival (ToA). Moreover, the dynamic positioning accuracy and measurement fail rate were evaluated in a closed indoor laboratory using the motion capture system as a reference system.

Materials and Methods

Structure of SSSLPS

The structure of the SSSLPS is shown in figure 1. Four speakers (FT28D, Fostex, Akishima, Tokyo, Japan) were set on the measurement area and connected to a PC through amplifiers (AP15d, Fostex) and an audio interface (OCTA-CAPTURE UA-1010, Roland Corp., Hamamatsu, Shizuoka, Japan) for converting analog signals to digital ones. The 3D printed cone shown in figure 2a was mounted on the speakers to emit omnidirectional sound, which also enables the area of coverage to be enlarged. The time division multiple access (TDMA) was applied to prevent interference between speakers (Segers et al., 2020). Each channel had a 250 ms time frame, and the period of emitting each channel SSSound (Spread Spectrum Sound) was 1 s (= 4 channels × 250 ms time frame). The audio interface also outputs a radio wave signal as the trigger signal at the beginning of the SSSound time frame by using the Zigbee device to obtain emitting time of the SSSound. The wireless SSSLPS receiving unit (fig. 2b) consists of a Field Programmable Gate Array (FPGA) board, an integrated sensor board, and a Jetson Nano processor, attaching two microphones (frequency response ± 3 dB, SPU0410LR5H-QB-7, Knowles Electronics, Itasca, Ill.) for recording the SSSound signals, Zigbee device to receive trigger signal.

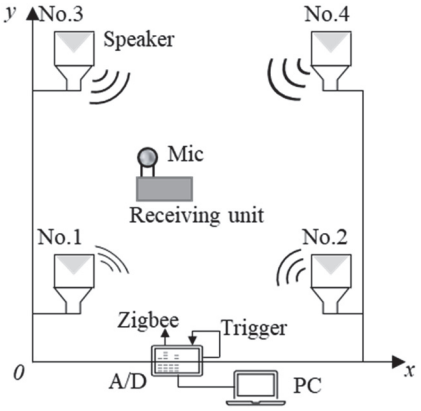

Figure 1. Structure of the positioning system.

The SSSound, $s(n)$, was generated by binary phase shift keying (BPSK) modulating with the pseudo random sequence, as shown in equation 1. In this research, M-sequences with 2047 length were used as persuading sequence in four channels. This modulation enabled noise tolerance and encoding security to the positioning system.

$$s(n) = \sin\left[\frac{2\pi f_{cj}(n)}{f_s}\right] \times M\left\{floor\left[\frac{f_{chip}(n)}{f_s}\right]\right\} \quad (1)$$

where n = 0, 1, 2 … 16376 (16376 = sampling frequency / chip rate × M-sequence length), M is vector of M-sequence, f_{cj} (Hz) is the carrier frequency of channel j, f_{chip} (cps) is the chip rate value, and f_s (Hz) is the sampling frequency. In the system, the carrier frequency, the chip rate, and the sampling frequency are 24 kHz, 12 kilo chip per second (kcps), and 96 kHz, respectively.

The sound signals and a trigger signal used different channels where each speaker has an individual channel. The trigger signal was synchronized at the beginning of the experiment. After the calibration of the signals, the UAV took off and started recording the sound. The cross-correlation and the position were calculated right after the equipment was stopped to check the validity of the experiment data.

Sound signals from speaker 1 and the trigger signal were emitted synchronously. After detecting the trigger signal in the receiver unit, the 0.25 second sound signal will be recorded, and the cross-correlation value is calculated by equation 2.

$$c(t) = \sum_{n=0}^{N-1} s(n)\, r(n+t) \quad (2)$$

where n = 0, 1, 2 … N - 1 (N is the sample length). t is the arrival time of the signal, $s(n)$ is the reference signal, $r(n)$ is

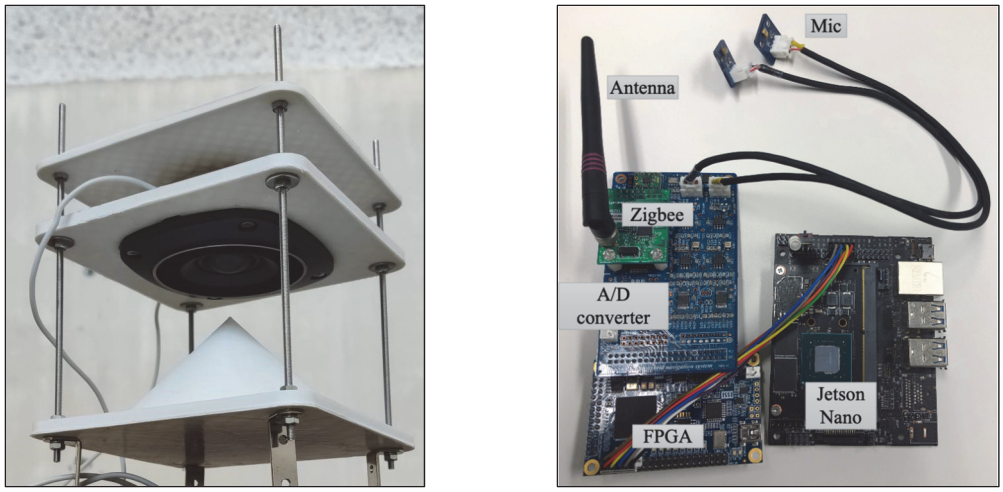

(a) (b)

Figure 2. (a) The speaker with a 3D printed cone and (b) hardware of the receiving unit.

the received signal. According to the calculated cross-correlation value, a normalized threshold calculated by equation 3, C_{th}, was used to distinguish a direct signal from reflected signals [12]:

$$C_{th} = C_{ave} + 4\sigma_{corr} \tag{3}$$

where C_{ave} and σ_{corr} are average absolute value and standard deviation of cross-correlation.

After getting the arrival time of SSSound, the distance d_j (m), from speaker to the microphone can be easily calculated by:

$$d_j = (331.5 + 0.61T) \times (t_j - t_t) \tag{4}$$

where T (°C) is the temperature at the microphone, t_j (s) is the arrival time of SSSound of channel j obtained by cross-correlation, and t_t (s) is the received time of the trigger signal.

The position of the microphone could be estimated by using a trilateration algorithm using at least three valid distances (Huang et al., 2020b). In this experiment, four distances were used to calculate position.

Doppler Shift Compensation

Previous Compensation Method

There are mainly two conventional Doppler shift compensation algorithms, one used an extra carrier wave to estimate the frequency shift (Amundson et al., 2008; Widodo et al., 2013), which occupied the power spectrum and led to a lower sound pressure level of an emitted signal. However, the extra carrier wave method is challenging to be applied to the UAV localization in a noisy environment. Another compensation algorithm extracts the carrier wave by digital signal processing (Tretter, 2008; Huang et al., 2021) (fig. 3). At first, the received signal $R(t)$ was filtered by a band-pass filter (BPF), then the signal was shifted into low frequency by multiplying a sine wave. The low-pass filter (LPF) cuts high-frequency noise. After that, a squaring function was used to remove M-sequence signals, and carrier wave frequency was detected by a fast Fourier transform (FFT). The Doppler shift was evaluated by the carrier wave. In this research, this previous algorithm was compared by extracting the carrier wave with the proposed method.

Proposed Compensation Algorithm

The proposed compensation algorithm uses an estimated frequency shift range calculated from the setting UAVs' moving velocity as the Doppler shift equation 5:

$$f_m = f_s \times \frac{v_s \pm v_r}{v_s}$$
$$\Delta f = f_m - f_s \tag{5}$$

where f_m (Hz) is the observed frequency, f_s (Hz) is the signal frequency, v_r (m/s) is the setting speed of the UAV viewed from the observer, v_s (m/s) is the speed of sound. Δf (Hz) is the estimated frequency shift, which would be a positive value if the source and observer are approaching each other, and would be negative if the observer is receding from the source. Since the objective is to control a UAV taking machine vision data at a moving speed of 200 mm/s, the resulting estimation of frequency shift range would be ±15 Hz. As a result, we choose to estimate the frequency shift from 23,985 to 24,015 Hz.

Figure 4 shows the proposed algorithm using frequency shift Ø (Hz) in the estimated frequency shift range (±15 Hz). Every time a given frequency shift Ø is used to generate the new carrier wave (carrier wave frequency is f_{cj} + Ø) multiplied with the M sequence based on an updated chip rate for

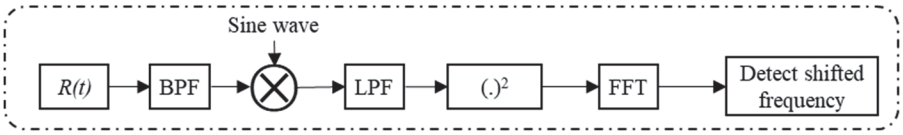

Figure 3. Block diagram of conventional Doppler compensation by extracting the carrier wave.

creating a new reference signal. In this experiment, an updated chip rate was defined as $f_{chip} = (f_{cj} + Ø) / 2$. The cross-correlation is calculated by using this new reference signal. In the case of that frequency shift step sets 1 Hz in the estimated frequency shift range (±15 Hz), a total of 31 cross-correlation waves are calculated. Among 31 cross-correlation waves, one cross-correlation wave is selected by the highest signal-to-noise ratio of correlation *SNRcorr* (eq. 6):

$$SNRcorr = 20 \log \frac{C_p}{C_m} \quad (6)$$

Where C_p is the maximum correlation value. C_m is the mean value of correlation. Higher *SNRcorr* value means that the reference signal used in correlation calculation is more similar to the received SSSound signal. The algorithm will judge the highest *SNRcorr* value as the correct correlation wave calculated using the correct frequency shift. The selected cross-correlation wave is used to measure the received time of SSSound by detecting its correlation peak. In this experiment, 1 Hz frequency shift step was mainly used, and 2 and 3 Hz frequency shift steps were used to evaluate the effective resolution of the frequency step.

Experiment

The experiment was conducted at Kyoto University, Uji Campus, Wind Tunnel Experiment Room on 17 February 2022. The test field (fig. 5a) consists of 4 speakers; its height was around 200 mm above the ground. The sound pressure level of each speaker was set to 100 dB and measured by a noise meter (LA-4440, frequency response ±1 dB, Ono Sokki, Kohoku-ku, Yokohama, Japan). A motion capture system (Accuracy 0.1 mm, Vicon, Centennial, Colo.), equipped with time-of-flight (ToF) cameras, was also set in the field to evaluate SSSLPS positioning accuracy (Merriaux et al., 2017). The measurement period of the motion capture system was 100 Hz and synchronized with SSSLPS using a trigger signal. A total station theodolite (Sokkia-SRX5XT32T-11) was set outside the experimental area to calibrate the motion capture and SSSLPS coordinate within 1.5 mm accuracy. We modified a UAV (Mavic Air, DJI, Nanshan, Shenzhen, China) by putting the printed circuit boards (PCBs) under the bottom part and attaching the microphones at the propeller guards next to the motion capture tracking markers (white dots) (fig. 5c). The moving path followed a 3 × 2 m path (fig. 5b). In this experiment, the coverage area was about 8 × 6 m, which was limited by the motion capture system. Previous research in a greenhouse using a static quadcopter with 9.75 N thrust shows the ability of SSSLPS for a 12 × 6 m coverage (Huang et al., 2020b). A typical solution for enlarging the coverage area is to use more speakers in the setup (Priyantha, 2005). Assuming the signal coverage for an SSSLPS on a quadcopter is 12 × 6 m, adding more speakers could increase the coverage area.

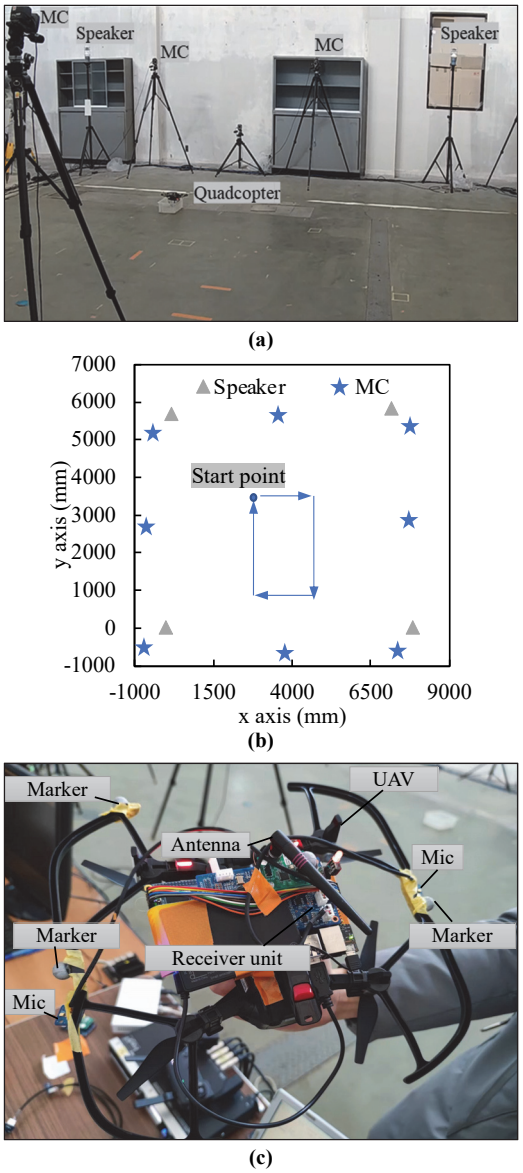

Figure 5. Experimental (a) test field where MC is motion capture (b) path plan with the location of (c) UAV.

The experiment conditions mimicked a greenhouse environment with a similar sound reflection index (Huang et al., 2021). Experiments in an indoor environment allowed for predicting the performance of the proposed algorithm for

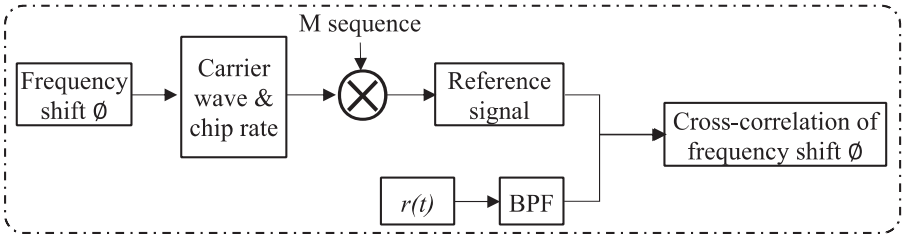

Figure 4. Block diagram of calculating cross-correlation at frequency shift Ø.

quadcopters in a greenhouse. As for the experiment setting, we set the UAV maneuvering speed at around 200 mm/s. This is because the objective of this project is to monitor plants with a machine vision system. As the experimental room's doors and windows were closed, there was no wind disturbance, and the temperature throughout the coverage area was relatively stable at 20°C. Experiments were replicated three times to evaluate the performance of the proposed algorithm. In this experiment, sound and trigger signals were just recorded by Jetson Nano of the receiver unit during UAV flying. Recorded data was post-processing by a PC (Core i5-6500, Intel, Santa Clara, Calif.).

Results and Discussion

Indoor UAV Flight Experiment

The position error of the proposed algorithm relative to the previous extracted algorithm in the three times experiments is shown in table 1. If the SNRcorr value (eq. 6) falls below 18 dB, which was determined from previous noise experiment results (Huang et al., 2020b), the distance measurement would be deemed a failure and could potentially provide an invalid ToA estimation. Fail rate means the number of failure measurements over the total measurements. Without any compensation, the average positioning failure rate was 90% and was only present in static positions. The fail rate of the previous extracted algorithm was 27.9% and much improved with Doppler shift compensation. This result found that a Doppler shift effect was significant for SSSLPS to measure UAV position. The proposed algorithm performs better than the previous extracted algorithm at a successful detection rate as the frequency shift estimation covers all possible frequency shifts. The 2D positioning error of using the proposed algorithm was 74.5 ± 37.6 mm, while using the previous extracted algorithm was 88.2 ± 60.2 mm.

In order to analyze in detail the performance of the proposed method in a single measurement, figure 6 shows an example of a measurement using the proposed system (SSLPS) and a motion capture (MC) system. This example has a 68.14 ± 34.06 mm 2D positioning error. In the absence of a compensation algorithm, it only has measurements for 8 out of a total of 94 measurements, and all the data verified are static measurements. Manually controlling the quadcopter leads to the path having a vibration during movement. Four ranging measurement results were shown in figure 7, and their corresponding means absolute errors were 86.1, 81.1, 92.3, and 81.6 mm, respectively. The mean absolute ranging error mainly affects the positioning accuracy (Huang et al., 2021). The proposed algorithm can reduce positioning errors with a smaller standard deviation value. These results indicate that the algorithm performs better than the previous extracted algorithm method of Doppler compensation, which guarantees the system could be used for a dynamic robot. The reasons will be discussed in the following sections 3.2 about UAV noise and sections 3.3 about the UAV velocity changes. To improve the overall performance of acoustic-based localization systems, hybrid positioning systems using other sensors, such as IMUs (Huang et al., 2017; Tientadakul et al., 2021) or ToF cameras (Paredes et al., 2017), can be considered. This research focused on improving the basic performance of the sound-based positioning system.

Table 1. Fail rate and 2D positioning error.

Method	Fail Rate (%)	Max Error (mm)	Min Error (mm)	Mean Error (mm)	Standard Deviation (mm)
Previous method	27.9	249.6	15.3	88.2	60.2
Spectrum peak algorithm	9. 8	206.3	18.6	74.5	37.6

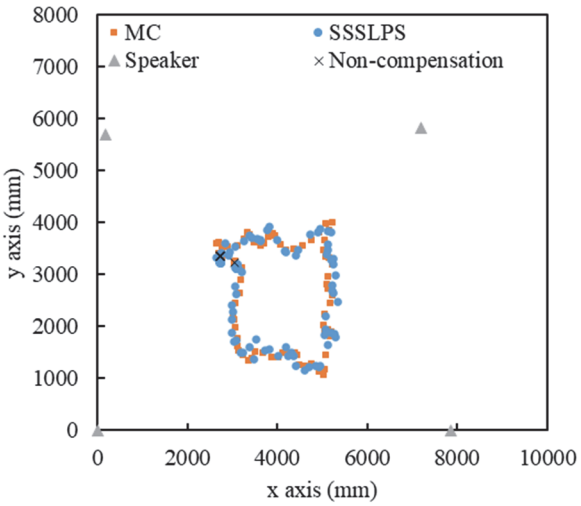

Figure 6. The 2D positioning measurement result.

Due to the high precision required by the positioning observation system, the optimal observation system as a reference is motion capture, and therefore the experiment needs to be conducted indoors (Huang et al., 2021). In a greenhouse, sound signals can be influenced by greenhouse walls, ground, and plants. The threshold processing method can handle reflected signals in greenhouses (Huang et al., 2020a; Shiigi et al., 2017). In addition, the experiments in this indoor environment had a stronger reflective index than in glass greenhouses, which means that a stronger reflected sound signal appeared in this experiment (heyizhou.net, 2018). In order to avoid plants in the acoustic path during system set-up, existing UWB studies should be consulted when conducting experiments in greenhouses where the transmitter and receiver are set on a different plane from the plants (De Preter et al., 2018; Yao et al., 2021). Compared to the indoor environment experiments in this study, the application in the greenhouse environment also requires greater coverage through a multi-speaker system (Smith et al., 2004).

Noise Effect

As the SSSLPS is an acoustic-based system, the operation of the UAV creates propeller noise and brushless motor noise issues over a wide bandwidth. A microphone (ECM-100N, Sony, Minato City, Tokyo, Japan) with a frequency response from 0 to 48 kHz of ± 3 dB and a noise meter (LA-4440, Ono Sokki, Addison, Ill.) with a frequency response in the hearing range of ± 1 dB were used to measure the acoustic noise spectrum of the quadcopter at the edge of the propeller, as reported in the previous research (Huang et al., 2020b). The recorded quadcopter noise, motor noise, and

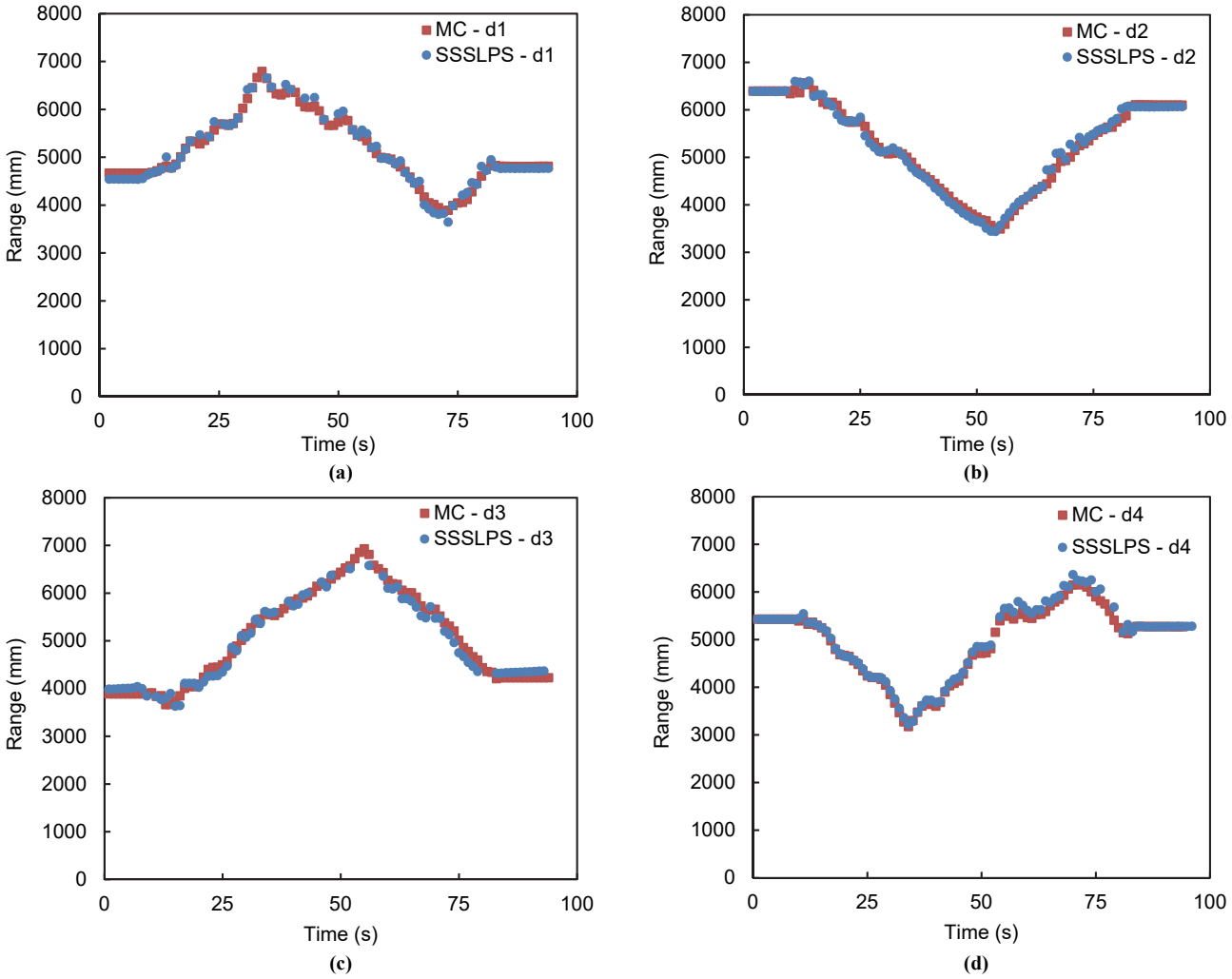

Figure 7. Ranging results of SSSLPS and motion capture from the microphone to (a) speaker 1 (b) speaker 2 (c) speaker 3 (d) speaker 4.

background environmental noise of our experiment are shown in figure 8a. Using the previous method in a noisy surrounding environment, the interfered carrier frequency is causing difficulties in finding the correct signal correlation. Thus, the calculated ToA would be inaccurate. The proposed method can tolerate the noise over a broad frequency spectrum and select a correct signal correction for calculating accurate ToA. Figure 8b is an example of a moving velocity of about 217.1 mm/s with the quadcopter noise. Usually, the carrier wave should only have one peak in the frequency spectrum (Huang et al., 2021). Due to high-frequency broadband noise interference caused by the quadcopter, extracting the carrier wave was challenging, which caused the previous algorithm to perform poorly. As a result, the positioning failure rate was 27.9%. The noise of the propeller and motor were distributed over a broad frequency range from around 83 and 64 dB in the same frequency range of SSSound, respectively. The proposed algorithm in this research estimated a series of possible frequency shifts to identify the most probable ToA with the highest cross-correlation. As a result, the proposed method was able to detect failure samples that could not be identified using the previous method due to the high-frequency broadband noise interference from a quadcopter.

Velocity Changes

The changing velocity during movement is another factor that can influence the Doppler shift compensation algorithm because the previous and proposed algorithm assumes the velocity is constant during movement (Widodo et al., 2013; Huang et al., 2021). However, in actual operation, the UAV will not only generate noise interference but will also have variations in velocity during movement. For the measurement example in figure 6, the momentary (0.01 s) maximum and average moving velocities are 378.3 and 121.5 mm/s by calculating MC measurement data separately. The average change of velocity during a signal length (0.171 s) was 49.1 mm/s^2. Figure 9a shows an example of the moving speed that has changed from 100 to 60 mm/s within a signal length. It shows that the UAV was decelerating during the distance measurement of the signal. During the experiment, the UAV moved at a changeable velocity (fig. 9b). Comparing the UGV experiment result (Huang et al., 2021), the UGV moved at a constant velocity with the change of velocity during a signal length was less than 20 mm/s^2 compared to over 40 mm/s^2 of UAV's (fig. 9b). It explains that the accuracy of the UAV (74.5 mm) is worse than the UGV (50.3 mm) because of a larger velocity change of the UAV.

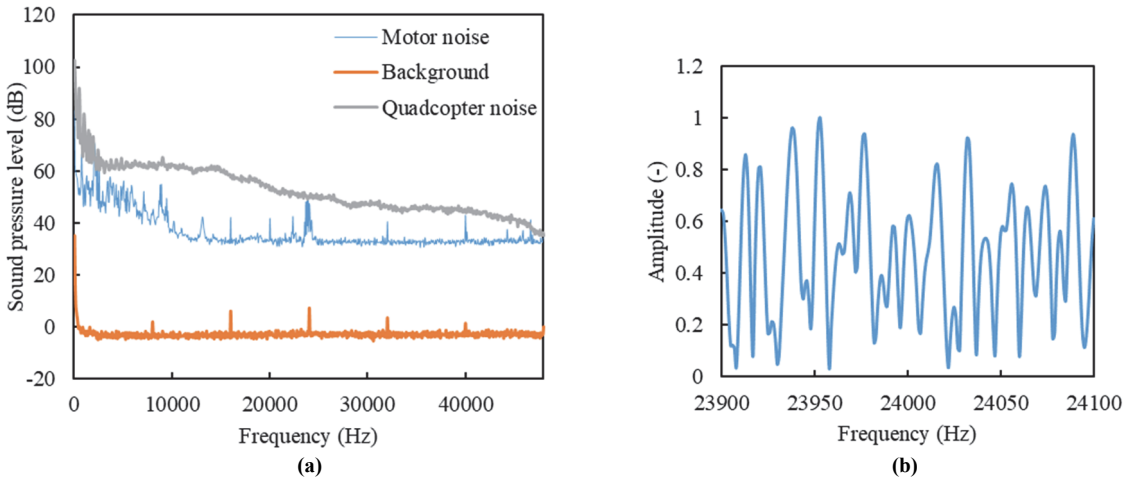

Figure 8. Examples of (a) acoustic noise spectrum, and (b) spectrum of acoustic signals around the carrier wave.

Frequency Steps Optimization

As a comparison, the above signal was successfully processed by the proposed algorithm. Results of the correlation from 23,985 to 24,015 Hz are shown in figure 10, where 24,011 Hz was the selected spectrum shift. From 24,009 to 24,014 Hz, the SNR was larger than 18 dB, and the SNR was below 18 dB for the other frequency shifts. To determine the optimal frequency steps of the algorithm, we can compare the computing costs and the failure rates of frequency steps of 2 and 3 Hz with 1 Hz. The selected process period measures the proposed Doppler compensation functions from loading the SSSound signals to calculating the correlation peak values so that the processing time could better reflect the actual computing time of different frequency steps. The CPU of Jetson nano is 1.4 GHz. With a 2 Hz step calculation, the Jetson Nano can process data within 1 s. However, due to the TDMA interval time, the measurement period is limited to 1 Hz, with a maximum measurement delay of 4 s. This may be too slow for navigation purposes when used for UAVs. To address this issue, we have proposed a hybrid navigation system that combines an IMU with the SSSLPS system (Tientadakul et al., 2021). The attainment of real-time computation can be facilitated by adoption of an IMU or a faster processor, which can potentially expedite the position calculation process at an accelerated pace.

Conclusions

The research objectives of this study were to address the noise and Doppler shift effect issues of a sound-based navigation system on a dynamically moving UAV, and to evaluate the proposed Doppler shift compensation algorithm for improving the accuracy and success rate of the SSSLPS. Through the conducted indoor UAV experiments in an 8 × 6 m area, the results indicate that the proposed algorithm can improve the accuracy of the SSSLPS to 74.5 ± 37.6 mm with a success rate of 90.2%, outperforming the accuracy of 88.2 ± 60.2 mm and success rate of 72.1% of the previous method. Furthermore, the proposed algorithm effectively enhances the success measurement rate and positioning accuracy of a dynamic quadcopter. The study also reveals that using frequency steps of 2 Hz in the algorithm can yield a

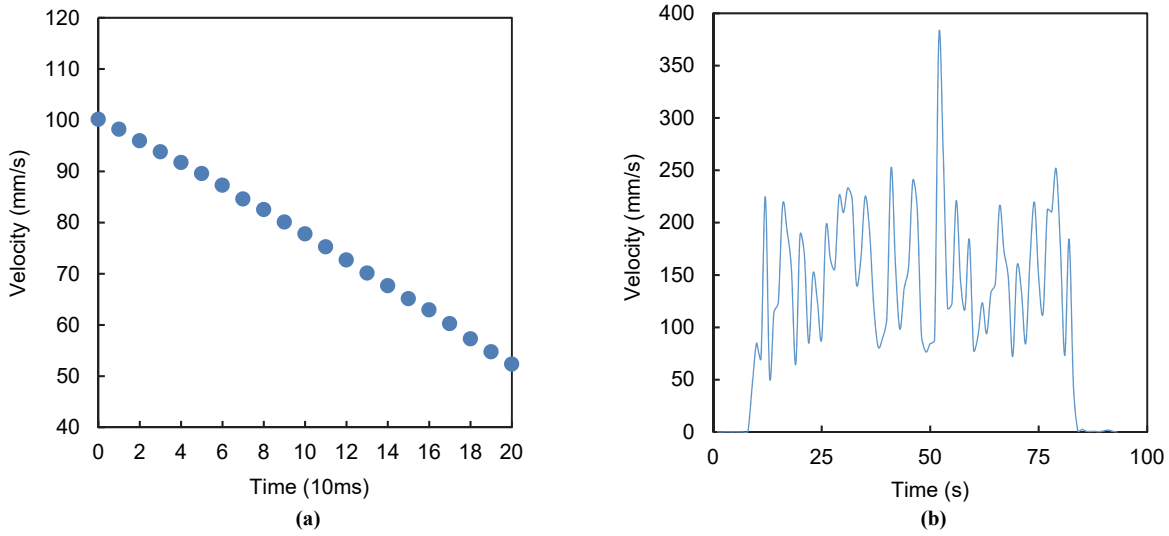

Figure 9. The velocity of UAV (a) within a signal transmission time and (b) the whole experiment.

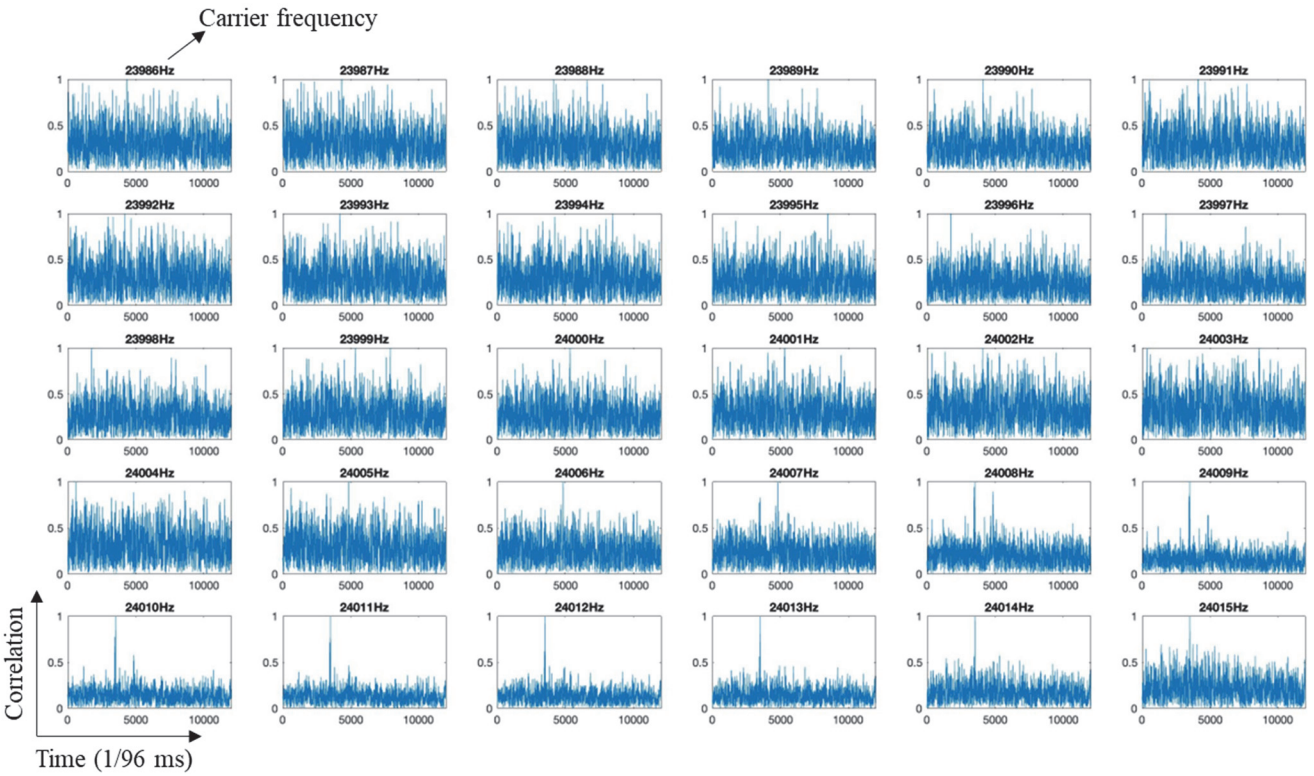

Figure 10. Correlation at different frequency shifts which 24011 Hz is the selected spectrum with the highest SNR.

better detection rate and calculation cost. However, the proposed algorithm requires computing resources when estimating the frequency shift of each SSSound signal.

In conclusion, this study has shown that the proposed SSSLPS has the potential to become a valuable positioning system with centimeter-level accuracy for guiding UAVs working in indoor fields such as warehouses or greenhouses. To apply the proposed system for positioning a quadcopter in a greenhouse, several challenges need to be addressed, such as enlarging the coverage area and achieving real-time positioning by employing sensor fusion methods along with an IMU. The current work, which was conducted in an indoor environment and involved post-processing of data, aims to develop a large-scale localization system to facilitate greenhouse robot operation in the future. Therefore, further research and development are needed to bridge the gap between the current system and its potential application in a real greenhouse environment, as well as to address the challenges that arise in scaling up the system for practical applications.

Acknowledgments

This research was supported by JSPS KAKENHI Grant Number 18H05364, and the Grant-in-Aid for JSPS Fellows with project number 22KF0179. The authors would like to thank Professor Garry John Piller of Kyoto University for proofreading this article.

References

Amundson, I., Koutsoukos, X., & Sallai, J. (2008). Mobile sensor localization and navigation using RF doppler shifts. *Proc. 1st ACM Int. Workshop on Mobile Entity Localization and Tracking in GPS-less Environments* (pp. 97-102). Association for Computing Machinery. https://doi.org/10.1145/1410012.1410034

De Preter, A., Anthonis, J., & De Baerdemaeker, J. (2018). Development of a robot for harvesting strawberries. *IFAC - PapersOnLine, 51*(17), 14-19. https://doi.org/10.1016/j.ifacol.2018.08.054

Gu, Y., Lo, A., & Niemegeers, I. (2009). A survey of indoor positioning systems for wireless personal networks. *IEEE Commun. Surv. Tutor., 11*(1), 13-32. https://doi.org/10.1109/SURV.2009.090103

heyizhou.net. (2018). Sound Absorption Coefficients. Retrieved from http://heyizhou.net/notes/absorption-coefficients

Huang, Z., Jacky, T. L., Zhao, X., Fukuda, H., Shiigi, T., Nakanishi, H.,... Kondo, N. (2020a). Position and orientation measurement system using spread spectrum sound for greenhouse robots. *Biosyst. Eng., 198*, 50-62. https://doi.org/10.1016/j.biosystemseng.2020.07.006

Huang, Z., Ono, M., Shiigi, T., Suzuki, T., Habaragamuwa, H., Nakanishi, H., & Kondo, N. (2017). Is spread spectrum sound a robust local positioning system for a quadcopter operating in a greenhouse? *Chem. Eng. Trans., 58*, 829-834. https://doi.org/10.3303/CET1758139

Huang, Z., Shiigi, T., Tsay, L. W., Nakanishi, H., Suzuki, T., Ogawa, Y., & Naoshi, K. (2021). A sound-based positioning system with centimeter accuracy for mobile robots in a greenhouse using frequency shift compensation. *Comput. Electron. Agric., 187*, 106235. https://doi.org/10.1016/j.compag.2021.106235

Huang, Z., Tsay, L. W., Shiigi, T., Zhao, X., Nakanishi, H., Suzuki, T.,... Kondo, N. (2020b). A noise tolerant spread spectrum sound-based local positioning system for operating a quadcopter in a greenhouse. *Sensors, 20*(7), 1981. https://doi.org/10.3390/s20071981

Krul, S., Pantos, C., Frangulea, M., & Valente, J. (2021). Visual SLAM for indoor livestock and farming using a small drone with a monocular camera: A feasibility study. *Drones, 5*(2), 41. https://doi.org/10.3390/drones5020041

Landolsi, M. A. (2017). Comparative analysis of delay-locked loop signal tracking for UWB systems. *Proc. 2017 4th Int. Conf. on Control, Decision and Information Technologies (CoDIT)* (pp. 144-148). IEEE. https://doi.org/10.1109/CoDIT.2017.8102581

Merriaux, P., Dupuis, Y., Boutteau, R., Vasseur, P., & Savatier, X. (2017). A study of Vicon system positioning performance. *Sensors, 17*(7), 1591. https://doi.org/10.3390/s17071591

Oppenheim, D., Edan, Y., & Shani, G. (2017). Detecting tomato flowers in greenhouses using computer vision. *Int. J. Comput. Inf. Eng., 11*(1), 104-109.

Paredes, J. A., Álvarez, F. J., Aguilera, T., & Villadangos, J. M. (2018). 3D indoor positioning of UAVs with spread spectrum ultrasound and time-of-flight cameras. *Sensors, 18*(1), 89. https://doi.org/10.3390/s18010089

Priyantha, N. B. (2005). The cricket indoor location system. PhD diss. Massachusetts Institute of Technology.

Ridolfi, M., Kaya, A., Berkvens, R., Weyn, M., Joseph, W., & De Poorter, E. (2021). Self-calibration and collaborative localization for UWB positioning systems: A survey and future research directions. *ACM Comput. Surv., 54*(4), 88. https://doi.org/10.1145/3448303

Roldán, J. J., Garcia-Aunon, P., Garzón, M., De León, J., Del Cerro, J., & Barrientos, A. (2016). Heterogeneous multi-robot system for mapping environmental variables of greenhouses. *Sensors, 16*(7), 1018. https://doi.org/10.3390/s16071018

Roldán, J. J., Joossen, G., Sanz, D., Del Cerro, J., & Barrientos, A. (2015). Mini-UAV based sensory system for measuring environmental variables in greenhouses. *Sensors, 15*(2), 3334-3350. https://doi.org/10.3390/s150203334

Sani, M. F., & Karimian, G. (2017). Automatic navigation and landing of an indoor AR.Drone quadrotor using ArUco marker and inertial sensors. *Proc. 2017 Int. Conf. on Computer and Drone Applications (IConDA)* (pp. 102-107). IEEE. https://doi.org/10.1109/ICONDA.2017.8270408

Segers, L., Braeken, A., & Touhafi, A. (2020). Optimizations for FPGA-based ultrasound multiple-access spread spectrum ranging. *J. Sens., 2020*, 4697345. https://doi.org/10.1155/2020/4697345

Shiigi, T., Kondo, N., Ogawa, Y., Suzuki, T., & Harshana, H. (2017). Temperature compensation method using base-station for spread spectrum sound-based positioning system in green house. *Eng. Agric. Environ. Food, 10*(3), 233-242. https://doi.org/10.1016/j.eaef.2017.03.004

Simon, J., Petkovic, I., Petkovic, D., & Petkovic, Á. (2018). Navigation and applicability of hexa rotor drones in greenhouse environment. *Tehnicki Vjesnik - Tech. Gazette, 25*(Suppl. 2). https://doi.org/10.17559/TV-20161109211133

Smith, A., Balakrishnan, H., Goraczko, M., & Priyantha, N. (2004). Tracking moving devices with the cricket location system. *Proc. 2nd Int. Conf. Mobile systems, applications, and services* (pp. 190-202). New York, N.Y.: Association for Computing Machinery. https://doi.org/10.1145/990064.990088

Tientadakul, R., Nakanishi, H., Shiigi, T., Huang, Z., Tsay, L. W., & Kondo, N. (2021). Spread spectrum sound with TDMA and INS hybrid navigation system for indoor environment. *J. Robot. Mechatron., 33*(6), 1315-1325. https://doi.org/10.20965/jrm.2021.p1315

Tretter, S. A. (2008). *Communication system design using DSP algorithms: With laboratory experiments for the TMS320C6713TM DSK.* Springer Science & Business Media.

Widodo, S., Shiigi, T., Hayashi, N., Kikuchi, H., Yanagida, K., Nakatsuchi, Y.,... Kondo, N. (2013). Moving object localization using sound-based positioning system with doppler shift compensation. *Robotics, 2*(2), 36-53. https://doi.org/10.3390/robotics2020036

Widodo, S., Shiigi, T., Than, N. M., Kikuchi, H., Yanagida, K., Nakatsuchi, Y.,... Kondo, N. (2014). Wind compensation for an open field spread spectrum sound-based positioning system using a base station configuration. *Eng. Agric. Environ. Food, 7*(3), 127-132. https://doi.org/10.1016/j.eaef.2014.04.001

Xiao, R., Du, H., Xu, C., & Wang, W. (2020). An efficient real-time indoor autonomous navigation and path planning system for drones based on RGB-D sensor. In Z. Deng (Ed.), *Proceedings of 2019 Chinese Intelligent Automation Conference* (pp. 32-44). Singapore: Springer. https://doi.org/10.1007/978-981-32-9050-1_4

Yan, Y., Zhang, B., Zhou, J., Zhang, Y., & Liu, X. (2022). Real-time localization and mapping utilizing multi-sensor fusion and Visual-IMU-Wheel odometry for agricultural robots in unstructured, dynamic and GPS-denied greenhouse environments. *Agronomy, 12*(8), 1740. https://doi.org/10.3390/agronomy12081740

Yao, L., Hu, D., Zhao, C., Yang, Z., & Zhang, Z. (2021). Wireless positioning and path tracking for a mobile platform in greenhouse. *Int. J. Agric. Biol. Eng., 14*(1), 216-223. https://doi.org/10.25165/j.ijabe.20211401.5627

Zhang, W., Gong, L., Huang, S., Wu, S., & Liu, C. (2022). Factor graph-based high-precision visual positioning for agricultural robots with fiducial markers. *Comput. Electron. Agric., 201*, 107295. https://doi.org/10.1016/j.compag.2022.107295